Pulse Intensity Coding Phase-Sensitive OTDR With Mismatched Filtering

Yaning Xie, Tuanwei Xu, Kai Cao, Jing Zhang, Dimin Deng, and Fang Li

***Abstract*—Optical pulse coding phase-sensitive optical time-domain reflectometry (Φ-OTDR) sends a series of pulses into the sensing fiber to enhance signal-to-noise ratio (SNR). And the spatial resolution is determined by the subpulse duration. The current challenges in optical pulse coding Φ-OTDR include long measurement time, complex coding design, and intricate modulation process. In this paper, pulse intensity coding and mismatched filtering is introduced, which could reach the theoretical measurement time determined by the fiber length. Additionally, it also simplifies coding design and modulation process. In order to obtain satisfactory decoding results, the least-squares criterion is used to design the mismatched filter. Experimental result demonstrates a 6.6 dB improvement in the SNR of the demodulated signal using a 10-bit coding pulse.**

***Index Terms*—Pulse coding, mismatched filtering, least-squares criterion, phase-sensitive optical time-domain reflectometry.**

I. Introduction

DISTRIBUTED optical fiber sensors (DOFS) have attracted a significant amount of attention around the world because of the outstanding advantages such as high flexibility and sensitivity, small size, intrinsically safe, long sensing distance and anti-electromagnetic interference [1], [2], [3]. A distributed sensor can realize distributed measurement of physical parameters such as temperature and strain changes [4], [5] by collecting and analyzing the specific scattered light at consecutive position along the fiber. As a representative distributed optical fiber sensing technology, phase-sensitive optical time-domain reflectometry (Φ-OTDR) utilizes Rayleigh backward scattering (RBS) light to detect and locate vibration signals, which has been extensively researched [6] and has demonstrated significant application potential in pipeline safety monitoring, perimeter security monitoring, oil and gas resource exploration, and natural seismic wave detection [7], [8], [9].

However, due to the relatively small Rayleigh scattering coefficient of the optical fiber, the amplitude of RBS light is usually weak, resulting in a low SNR of the demodulated signal, which will affect the reliability of vibration measurement [10]. To address the problem, chirped pulse scheme is proposed. It sends a long pulse with frequency chirp to the sensing fiber. Compared to a single short duration pulse, chirped pulse increase the pulse width, thereby enhancing the energy of the injected pulse and ultimately improving the SNR of the detected signal. After compression with matched filter, the chirped pulse's width shortens, leading to an improved spatial resolution comparable to that of a single short pulse. In 2019, Wang et al. applied linear frequency modulation (LFM) pulse in coherent detection Φ-OTDR, achieving vibration measurement over a 10 km sensing fiber with 0.9 m spatial resolution [11]. Subsequently, in 2020, Zhe et al. employed digital LFM pulse in coherent detection Φ-OTDR, enabling actual acoustic sensing at frequencies of 1.5 kHz and 3 kHz through SNR enhancement [12]. However, the spatial resolution is inversely proportional to the sweep frequency range, requiring a complex modulation process and increasing overall system complexity significantly.

Moreover, pulse coding is a proven scheme in Φ-OTDR system. In 2016, the cyclic pseudorandom binary sequence (PRBS) was introduced into Φ-OTDR in a 500 m fiber with 2.5 cm spatial resolution [13]. However, the scan rate, which is the reciprocal of the measurement time, can only achieve ∼60% of the theoretical limit. In 2018, near perfect periodic autocorrelation (PPA) codes based on biphasic Legendre sequences were introduced, achieving a spatial resolution of 14.7 cm in a 1 km fiber [14]. However, owing to the long coding sequence in pursuit of a better peak to sidelobe level (PSL), the scan rate was lower than 21% of the theoretical limit. The scan rate of these schemes is far from the theoretical limit because of the long coding sequence. Apart from the scan rate issue, a 90-degree optical hybrid is needed in all above schemes for decoding, which increases the complexity and cost of the system. In addition, the coherent detection Φ-OTDR based on Golay codes has had significant advancements in recent years. Bipolar orthogonal complementary Golay codes, employing a decoding process based on Jones matrix estimation, have achieved ∼25%

Manuscript received 16 February 2024; revised 20 April 2024; accepted 5 May 2024. Date of publication 9 May 2024; date of current version 17 May 2024. This work was supported in part by the National Key R&D Program of China under Grant 2023YFC3010703, in part by the Research Program of Sanya Yazhou Bay Science and Technology City under Grant SKJC-2020-01-009, and in part by the Strategic Priority Research Program of the Chinese Academy of Sciences under Grant XDA22040105. *(Corresponding authors: Tuanwei Xu; Fang Li.)*

Yaning Xie and Jing Zhang are with the State Key Laboratories of Transducer Technology, Institute of Semiconductors, Chinese Academy of Sciences, Beijing 100083, China, and also with the School of Electronic, Electrical and Communication Engineering, University of Chinese Academy of Sciences, Beijing 100049, China (e-mail: xieyaning@semi.ac.cn; zhangjing01@semi.ac.cn).

Tuanwei Xu, Kai Cao, and Fang Li are with the State Key Laboratories of Transducer Technology, Institute of Semiconductors, Chinese Academy of Sciences, Beijing 100083, China, and also with the College of Materials Science and Opto-Electronic Technology, University of Chinese Academy of Sciences, Beijing 100049, China (e-mail: xutuanwei@semi.ac.cn; caokai@semi.ac.cn; lifang@semi.ac.cn).

Dimin Deng is with the State Key Laboratories of Transducer Technology, Institute of Semiconductors, Chinese Academy of Sciences, Beijing 100083, China (e-mail: ddm911@semi.ac.cn).

Digital Object Identifier 10.1109/JPHOT.2024.3399055

of the theoretical scan rate limit [15]. A linearized optical pulse coding Φ-OTDR with unipolar Golay codes probe pulses can be realized by heterodyne detection and bandpass filtering [16], without necessarily needing a 90-degree optical hybrid. Bipolar Golay codes probe pulses have been employed in a 10 km fiber with 0.92 m spatial resolution, achieving ∼50% of the theoretical scan rate limit [17]. The scan rate of these schemes falls below the theoretical limit, as multiple rows of coding sequences are required to complete the decoding procedure. Furthermore, the sensing bandwidth is considerably reduced due to the low scan rate.

To solve the scan rate issue mentioned above, the random coding is introduced. In 2022, Li et al. employed random coding pulse in coherent detection Φ-OTDR, achieving 14.19 dB SNR improvement using 128-bit random coding pulse [18]. In this scheme, the coding sequence is randomly generated, and the decoding sequence is obtained by subtracting its mean from the coding sequence. Only a single row of coding sequence is required for completing measurement, maintaining the original sensing bandwidth. However, in order to achieve a better PSL, this scheme demands a high degree of randomness in the coding sequence, necessitating the use of a physical random number generator. Undoubtedly, this raises both the cost and complexity of the system. Simultaneously, Liang et al. introduced mismatched filtering and phase coding into Φ-OTDR [19]. This technology mitigates the need for a high degree of randomness in the coding sequence, making it easy to achieve a good PSL. However, this scheme involves modulating the phase, which needs a complex modulation process.

In this paper, a pulse intensity coding Φ-OTDR with mismatched filtering is proposed. The scheme requires only a single sequence to complete the measurement, which means it can bring SNR enhancement without loss of the sensing bandwidth. Simultaneously, the scheme mitigates the requirement for a high degree of randomness in the coding sequence and eliminates the need for a complex modulation process. Compared with the single pulse under the same conditions, the SNR of the demodulated signal is improved by 6.6 dB using a 10-bit coding pulse. Furthermore, we also analyzed the spatial resolution of the system. Prior to analyzing spatial resolution, the interference fading is suppressed by using spectrum extraction [20] and rotated-vector-sum method [21]. Based on the experimental results, the spatial resolution is close to 100 m without mismatched filtering. After mismatched filtering, the spatial resolution is restored to 13 m, demonstrating the effectiveness of utilizing mismatched filter for decoding. The value is slightly larger than the theoretical value of 10 m because the process of eliminating interference fading compromises the spatial resolution.

II. Principle

A. Pulse Intensity Coding in Coherent Detection Φ-OTDR System

In a representative Φ-OTDR system with coherent detection, a small part of the light emitted by a ultra-narrow linewidth laser is allocated as a local oscillator (LO) light. Most of the light is modulated into pulsed light and injected into the sensing fiber, resulting in the RBS light due to the fluctuated refractive index distribution along the fiber. The RBS signal $E_{RBS}(t)$ and the LO light $E_{LO}(t)$ can be expressed as:

$$E_{RBS}(t) = A_R(t)cos[\omega_R t + \varphi_R + \varphi(t)] \tag{1}$$

$$E_{LO}(t) = A_{LO}cos(\omega_{LO} t + \varphi_{LO}) \tag{2}$$

where $A_R(t)$ and $\varphi(t)$ are the amplitude and phase of the RBS signal respectively. ω_R and φ_R represent the angular frequency and the initial phase of the pulsed light. A_{LO}, ω_{LO} and φ_{LO} are the amplitude, the angular frequency and the initial phase of the LO light respectively.

Then the beating signal can be obtained by mutual interference between the RBS light and the LO light. After removing the DC component and digitally down-converted into baseband, the beating signal can be described as:

$$I(t) = rA_R(t)A_{LO}cos[\varphi_d + \varphi(t)] \tag{3}$$

where r is the response factor of the photodetector employed in the system, $\varphi_d = \varphi_R - \varphi_{LO}$. The amplitude $A_R(t)$ and the phase $\varphi(t)$ can be obtained through the following equations:

$$A_R(t) \propto \sqrt{I^2(t) + Q^2(t)} \tag{4}$$

$$\varphi(t) \approx \text{angle}[I(t) + iQ(t)] - \varphi_d \tag{5}$$

where $Q(t)$ is the quadrature signal of $I(t)$, which can be obtained by Hilbert transform [22], and i is the imaginary unit. After demodulating $A_R(t)$ and $\varphi(t)$, valuable information regarding external vibrations along the fiber can be extracted.

The pulse intensity coding Φ-OTDR injects a series of pulses into the sensing fiber instead of a single pulse. Assuming that a pulse intensity coding sequence $C = [C_1, C_2, C_3, \ldots, C_L]$ with the coding length of L bits is expressed as:

$$\hat{C} = \sum_{n=1}^{L} C_n \exp(i\omega_R n\tau)\, \text{rect}(t - n\tau) \tag{6}$$

where C_n represents the amplitude of the n-th pulse and $rect()$ is a rectangular function with time duration of τ.

Although the RBS signal undergoes slow variations due to the changes in the external environment and the operational state of the laser, the measurement time of a single RBS signal in dynamic measurement is much smaller than the timescale of external environmental changes or laser state changes. Therefore, the entire Φ-OTDR system can be considered as a natural linear-time-invariant system. The RBS signal of the pulse sequence is the sum of the RBS signal of each pulse inside the sequence and it can be described as:

$$\begin{aligned} E'_{RBS}(t) &= \sum_{n=1}^{L} C_n \exp(i\omega_R n\tau)\, E_{RBS}(t - n\tau) \\ &= \sum_{n=1}^{L} C_n A_R(t - n\tau) \exp[i\omega_R t + i\varphi_R + i\varphi(t - n\tau)] \end{aligned} \tag{7}$$

When the RBS light interferes with the LO light, the generated beating signal is:

$$I_{\text{code}}(t) = \sum_{n=1}^{L} rC_n A_R(t-n\tau)A_{LO}\cos\left[\Delta\omega t + \varphi_d + \varphi(t-n\tau)\right] + \sum_{n=1}^{L-1}\sum_{m=n+1}^{L} 2rC_nC_mA_R(t-n\tau)A_R(t-m\tau)cos(\varphi_{nm}) \tag{8}$$

where $\varphi_{nm} = \varphi(t-n\tau) - \varphi(t-m\tau)$.

The beating signal can be divided into two parts: the first part is the sum of beating signals generated by the mutual interference between the RBS light from each pulse in the pulse sequence and the LO light; the second part is the crosstalk term generated by the mutual interference between the RBS light from different pulses in the pulse sequence.

When the coding length is relatively short, the crosstalk term is negligible because the value of A_R is much smaller than that of A_{LO}. However, when the coding length is long enough, the crosstalk term cannot be ignored. Nevertheless, referring to (8), it can be noted that the crosstalk term falls within a low frequency band, different from the frequency band of the beating signal. The impact of the crosstalk term can be eliminated by a Finite Impulse Response (FIR) filter. After band-pass filtering and digital down-conversion, the beating signal can be expressed as:

$$\begin{aligned} I_{\text{code}}(t) &= \sum_{n=1}^{L} rC_nA_R(t-n\tau)A_{LO}\cos\left[\varphi_d + \varphi(t-n\tau)\right] \\ &= \sum_{n=1}^{L} I(t-n\tau)C_n = I(t) * C \end{aligned} \tag{9}$$

where the operator $*$ represents the convolution operation. According to (9), the system response of the coding pulse is the convolution of the single pulse response and the coding sequence. The single pulse response can be restored by proper decoding method. After decoding, the amplitude and the phase of the RBS light can be demodulated by (4) and (5).

B. Decoding With Mismatched Filtering

Mismatched filtering has been applied to radar and has been investigated extensively. Especially, mismatched filtering can be used to obtain a satisfactory PSL when a short coding pulse is used. When the beating signal $I_{code}(t)$ is decoded by the mismatched filter $h(t)$, the decoded signal $I_d(t)$ is given by:

$$I_d(t) = I_{\text{code}}(t) \otimes h(t) \tag{10}$$

where the operator $\otimes$ represents the cross-correlation operation. $h(t)$ can be expressed as:

$$h(t) = \sum_{n=1}^{M} \left[h_n \cdot \delta(t-(n-1)\tau)\right] \tag{11}$$

where h_n represents the decoding sequence. The length of decoding sequence is generally longer than that of coding sequence, which is different from matched filtering.

To illustrate the design of h_n, we substitute (9) into (10) and the result is:

$$I_d(t) = I(t) \otimes h_d(t) \tag{12}$$

where $h_d(t) = C \otimes h(t)$ is the decoded pulse after mismatched filtering.

In the following part, the detailed derivation of mismatched filtering based on the least-squares criterion will be presented. According to the cross-correlation properties, we can get:

$$C \otimes h(t) = \sum_{n=1}^{L+M-1} \left[b_n \cdot \delta(t-(n-1)\tau)\right] \tag{13}$$

where b_n is the discrete cross-correlation of C_n and h_n. Each value of b_n can be characterized as follows:

$$b_n = \begin{bmatrix} C_{n-M+1} & C_{n-M+2} & \cdots & C_n \end{bmatrix} \begin{bmatrix} h_1 \\ h_2 \\ \vdots \\ h_M \end{bmatrix} \tag{14}$$

where $n = 1, 2, \ldots, L+M-1$, the vector $[C_{n-M+1}, C_{n-M+2}, \ldots, C_n]$ is formed from C_n. It is important to note that, if $n \le 0$ and $n \ge L+1$, then $C_n = 0$. After simple derivation, (14) can be expressed in matrix form:

$$b = Xh \tag{15}$$

where the vector $b = [b_1, b_2, \ldots, b_{L+M-1}]^T$ and $h = [h_1, h_2, \ldots, h_M]^T$ represents the decoding vector. When cross-correlating C_n and h_n, the desired outcome is a single peak at the central position with no sidelobes elsewhere. Consequently, the constraint on b_n is such that it has a value of 1 at the $(M+L)/2$ element and 0 elsewhere. The matrix X is a Toeplitz matrix formed by C_n and can be expressed as:

$$X_{(L+M-1)M} = \begin{bmatrix} 0 & 0 & \cdots & C_1 \\ 0 & \cdots & C_1 & C_2 \\ \vdots & \vdots & \vdots & \vdots \\ C_L & 0 & \cdots & 0 \end{bmatrix} \tag{16}$$

Equation (15) has a least-squares solution, which is:

$$\widehat{h_n} = \left(X^H X\right)^{-1} X^H b_n \tag{17}$$

where $\widehat{h_n}$ is the designed decoding sequence. So far, the design of the mismatched filter has been completed. The single pulse response can be obtained by decoding the beating signal using the mismatched filter.

III. Experiment Analysis and Discussion

A. Experimental System

The experimental setup of the coherent detection Φ-OTDR system with pulse intensity coding is shown in Fig. 1 . A narrow linewidth laser (RIO0175-3-34-3) was used in the experiment, emitting continuous light characterized by a linewidth of 1.8 kHz

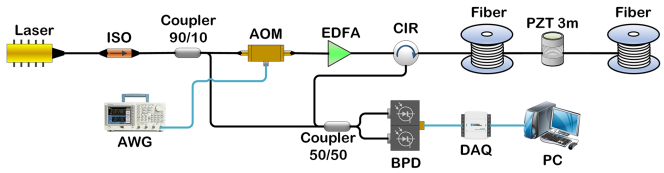

Fig. 1. Experimental setup of Φ-OTDR.

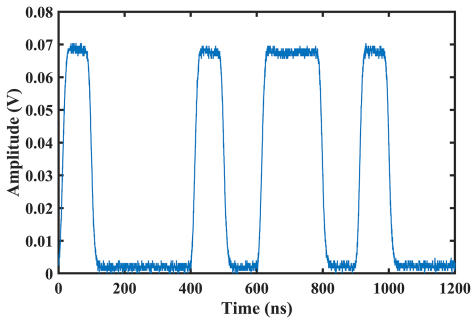

Fig. 2. The time domain waveform of the probe signal.

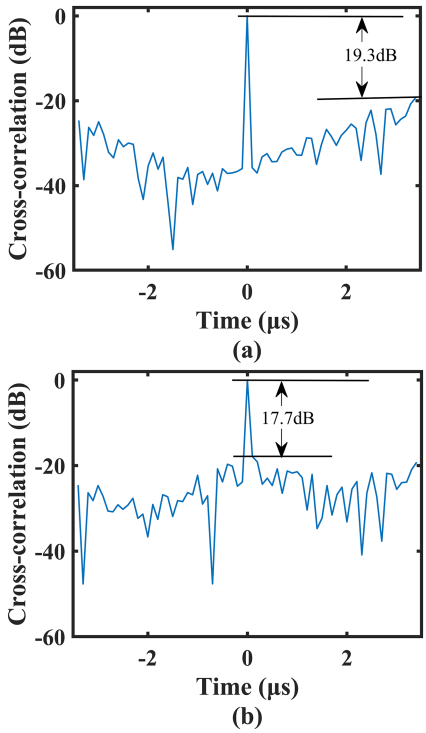

Fig. 3. The cross-correlation between the coding sequence and the decoding sequence (a) under ideal conditions (b) under actual conditions.

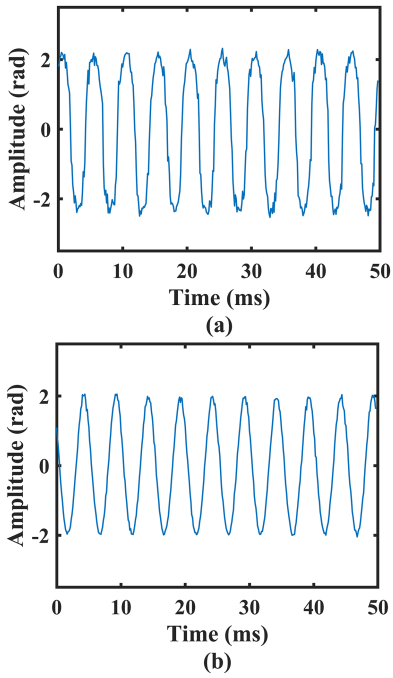

Fig. 4. The temporal waveform of vibration signal (a) for the single pulse (b) for the coding pulse.

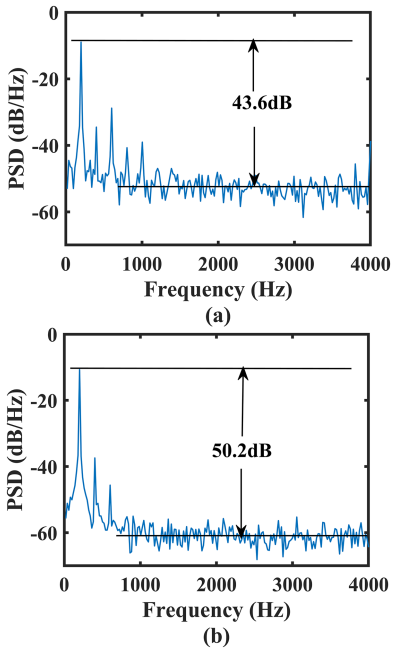

Fig. 5. (a) The PSD for the single pulse (b) The PSD for the coding pulse.

and a center wavelength of 1550.12 nm. After an isolator (ISO) and a 90:10 beam splitter, 90% of the laser was used as the probe light, and 10% was the LO light. The probe was modulated into coding pulse by an acousto-optic modulator (AOM: SGTF200-1550-1T-2A1) with a 200 MHz frequency shift. The pulse repetition rate is 8 kHz. The AOM was driven by an arbitrary waveform generator (AWG: SDG7102 A) to produce a series of pulses according to the coding sequence. Subsequently, the pulsed light was amplified by an erbium-doped fiber amplifier (EDFA: BG-pulse-EDFA-M-20W-1550-FC/APC) to get a suitable peak power. Then the pulsed light was injected into a 9 km sensing fiber through a circulator (CIR). We placed a piezoelectric ceramic transducer (PZT) at about 4.8 km, which was driven by a sinusoidal signal with an amplitude of ± 1 V and a frequency of 200 Hz. The collected RBS light was coupled with the LO light through a 50:50 coupler. And the combined optical signal was converted into electrical signal by a balanced photodetector (BPD: UBD-1.2G-A) with a 1.2-GHz bandwidth. The electrical signal was sampled by a data acquisition (DAQ:

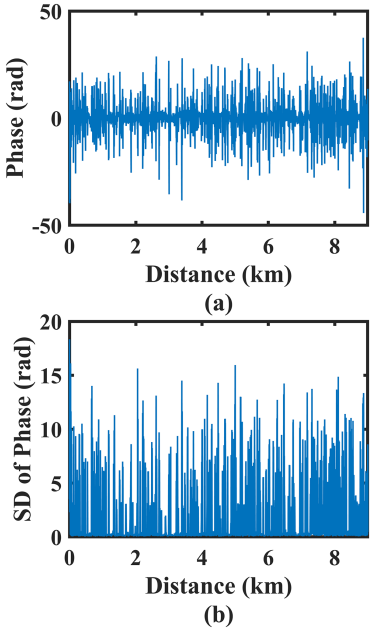

Fig. 6. (a) The 100 differential phase traces (b) The standard deviation of these differential phase traces.

NI PXIe-5160) card with a sampling rate of 1250 MS/s. Finally, the collected signal was sent to a computer for subsequent digital signal process.

B. Experimental Results and Analysis

In the experiment, the use of mismatched filtering eliminates the need for a high degree of randomness in the coding sequence. So the coding sequence can be directly generated by the computer randomly without more complex methods. Certainly, not any sequence randomly generated by the computer can serve as a coding sequence. When designing coding sequence, two factors need to be considered: the PSL obtained by cross-correlating the coding sequence with its corresponding decoding sequence and transient effects in EDFA. For the PSL, the larger the value, the more favorable it is for decoding; otherwise, it is less favorable for decoding. Transient effects in EDFA can adversely impact the implementation of the coding pulse Φ-OTDR, especially when the length of coding pulse is excessively long or the driving current for EDFA is set too high. Transient effects can result in inconsistent power levels of the pulses in the pulse sequence after amplifying by EDFA. In order to mitigate the transient effects, the length of the coding pulse is 10 bits with a subpulse width of 100 ns and the driving current for the EDFA is configured at a relatively low level. Additionally, a more uniform distribution of 0 and 1 in the coding sequence is advantageous for mitigating the transient effects. Fig. 2 shows the time domain waveform of the probe signal, illustrating relatively consistent power levels for each pulse in the pulse sequence, aligning well with the design requirement.

According to the least-squares criterion, we designed the decoding sequence by mismatched filtering. To achieve a satisfactory PSL, the length of the decoding sequence is set at 60 bits, six

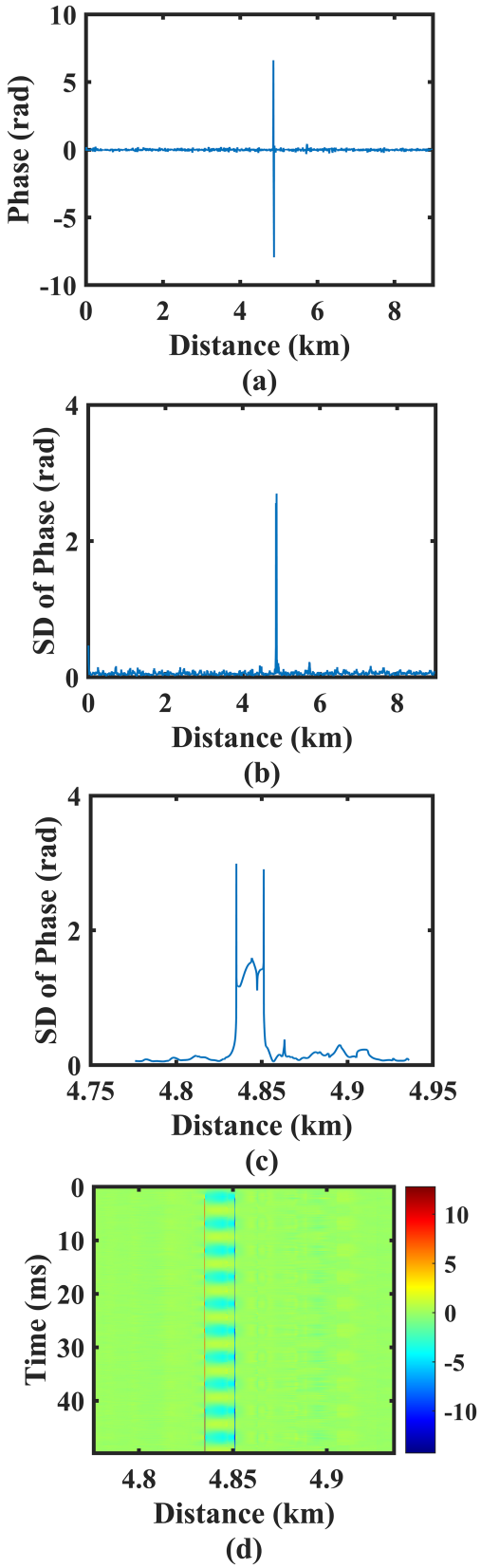

Fig. 7. With mismatched filtering and after eliminating interference fading (a) The 100 differential phase traces (b) The standard deviation of these differential phase traces (c) The local zoom-in near the vibration region from (b) (d) The spatiotemporal map around the vibration region.

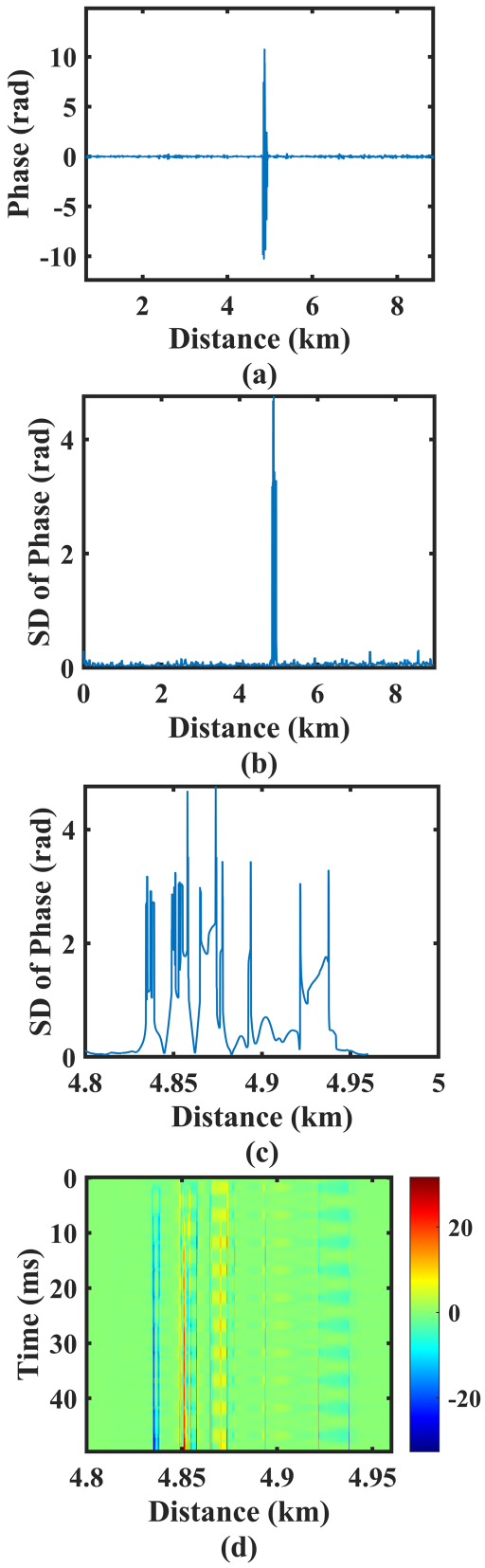

Fig. 8. Without mismatched filtering and after eliminating interference fading (a) The 100 differential phase traces (b) The standard deviation of these differential phase traces (c) The local zoom-in near the vibration region from (b) (d) The spatiotemporal map around the vibration region.

times the length of the coding sequence. The cross-correlation result between the coding sequence and the decoding sequence is presented in Fig. 3(a), showing a PSL of 19.3 dB under ideal conditions. However, in practical scenarios, slight variations in the power of individual pulses within the pulse sequence can affect the PSL. We collected the power values of individual pulses in the pulse sequence under actual conditions and performed cross-correlation with the decoding sequence. The result is shown in Fig. 3(b), the PSL is 17.7 dB, slightly lower than the ideal value. Nevertheless, subsequent experimental results prove that even with a PSL of 17.7 dB, satisfactory results can still be achieved.

Then we assessed the SNR improvement when using coding pulse. In the experiment, the peak power of the coding pulse is set equal to that of the single pulse. For the single pulse Φ-OTDR, after collecting the beating signal from BPD, Hilbert demodulation is performed. Then the retrieved temporal waveform of external vibration signal can be acquired. The result is presented in Fig. 4(a). For the coding pulse Φ-OTDR, the raw signal collected from the BPD firstly undergoes band-pass filtering and digital down-conversion processing. Subsequently, according to the sampling rate and pulse width, resampling is applied to the signal [23]. The resampled signal is then decoded by cross-correlation with the decoding sequence. Finally, after Hilbert demodulation process, the time-domain waveform of external vibration signal can be recovered. And the result is demonstrated in Fig. 4(b). By comparing Fig. 4(a) and (b), it is evident that the coding pulse can reduce the noise and the temporal waveform of the vibration signal can be retrieved more accurately. The corresponding power spectral density (PSD) is presented in Fig. 5. The PSD has a peak at 200 Hz, which is the frequency of the applied sinusoidal signal. The SNR of the demodulated signal is calculated in the PSD by taking the difference between the signal peak and average noise level which is far from the peak. For the single pulse, the SNR is 43.6 dB. Whereas for the coding pulse, the SNR is 50.2 dB. Compared to the single pulse, the SNR is improved by 6.6 dB. This implies the coding pulse Φ-OTDR we proposed is effective in improving the SNR of the demodulated signal.

In order to analyze the spatial resolution of the coding pulse Φ-OTDR, the 100 differential phase traces and the corresponding standard deviation (SD) of these differential phase traces are presented in Fig. 6(a) and (b), respectively. However, due to the presence of interference fading, the vibration signal is submerged in noise, making it challenging to accurately analyze the spatial resolution. Therefore, it is essential to eliminate interference fading before analyzing the spatial resolution. The interference fading is primarily caused by the long coherence length laser. The mainstream method for mitigating interference fading involves superimposing multiple degrees of freedom [24]. In this paper, we employ spectrum extraction [20] and rotated-vector-sum method [21] to suppress interference fading. We utilized FIR band-pass filters to extract three frequency bands: 180 MHz to 200 MHz, 190 MHz to 210 MHz and 200 MHz to 220 MHz.

The results after eliminating interference fading are presented in Fig. 7. Fig. 7(a) displays the 100 differential phase traces.

Compared to Fig. 6(a), almost all fading points were eliminated. In general, we can assess the effectiveness of eliminating interference fading by calculating the proportion of fading points. Regarding interference fading, there is no universal standard for the definition of fading points. In many investigations, the fading positions are regarded as those points whose RBS intensities are lower than 20% of the mean value. The percentage of fading points is 4.16% in the original signal, decreasing to 0.45% after eliminating interference fading, implying the effect of eliminating interference fading is very good. Fig. 7(b) displays the standard deviation of the 100 differential phase traces, Fig. 7(c) provides a local zoom-in near the vibration region from Fig. 7(b) and 7(d) illustrates a spatiotemporal map around the vibration region. From Fig. 7(c), we can obtain that the spatial resolution of the system is 13 m, which aligns well with Fig. 7(d). It is slightly larger than the theoretical spatial resolution of 10 m, which is determined by the 100 ns pulse width of the subpulse. This is because the interference fading suppressing algorithm tends to slightly increase the spatial resolution.

As a comparison, we assessed the spatial resolution of the system without employing mismatched filter for decoding to validate the effectiveness of the decoding algorithm. The results are presented in Fig. 8. Before analyzing the spatial resolution, the interference fading was also mitigated. Fig. 8(a)–(d) correspond one-to-one with Fig. 7(a)–(d). From Fig. 8(c), we can obtain the spatial resolution of the system is 100 m, consistent with the 1000 ns pulse width of the coding pulse. Fig. 8(d) also supports this result. By comparing the spatial resolution of the system before and after decoding, it is evident that this decoding method is successful and effective.

IV. Conclusion

In this paper, a pulse intensity coding Φ-OTDR with mismatched filtering is proposed. The scheme requires only a single sequence to complete the measurement, maintaining the original sensing bandwidth. In addition, the scheme mitigates the requirement for a high degree of randomness in the coding sequence and eliminates the need for a complex modulation process. Compared with the single pulse under the same conditions, the SNR of the demodulated signal is improved by 6.6 dB using a 10-bit coding pulse. In order to analyze the spatial resolution, the interference fading is suppressed by the spectrum extraction and rotated-vector-sum method. Without mismatched filtering, the spatial resolution is close to 100 m. After mismatched filtering, the spatial resolution is restored to 13 m, demonstrating the effectiveness of utilizing mismatched filter for decoding. More advanced mismatched filter designs are worthy of further investigation to achieve higher performance.

References

[1] P. S. Westbrook et al., "Continuous multicore optical fiber grating arrays for distributed sensing applications," *J. Lightw. Technol.*, vol. 35, no. 6, pp. 1248–1252, Mar. 2017.

[2] H. Yuan et al., "An anti-noise composite optical fiber vibration sensing system," *Opt. Lasers Eng.*, vol. 139, 2021, Art. no. 106483.

[3] A. Barrias, J. R. Casas, and S. Villalba, "A review of distributed optical fiber sensors for civil engineering applications," *Sensors*, vol. 16, no. 5, 2016, Art. no. 748.

[4] A. Masoudi et al., "Dynamic strain measurement in subsea power cables with distributed optical fibre vibration sensor," in *Proc. Adv. Photon. (BGPP, IPR, NOMA NP, Sensors, Netw., SPPCom, SOF)*, 2018, Paper SeTh2E.1. [Online]. Available: https://opg.optica.org/abstract.cfm?URI=Sensors-2018-SeTh2E.1

[5] G. Dai, X. Fan, and Z. He, "A long-range fiber-optic raman distributed temperature sensor based on dual-source scheme and RZ simplex coding," in *Proc. IEEE Asia Commun. Photon. Conf.*, 2018, pp. 1–3.

[6] Y. Shang et al., "Research progress in distributed acoustic sensing techniques," *Sensors*, vol. 22, no. 16, 2022, Art. no. 6060.

[7] Z. Zhang, X. Fan, and Z. He, "Long-range distributed static strain sensing with <100 nano-strain resolution realized using OFDR," *J. Lightw. Technol.*, vol. 37, no. 18, pp. 4590–4596, Sep. 2019.

[8] M. Wu, X. Fan, Q. Liu, and Z. He, "Quasi-distributed fiber-optic acoustic sensing system based on pulse compression technique and phase-noise compensation," *Opt. Lett.*, vol. 44, no. 24, pp. 5969–5972, 2019.

[9] Q. He, T. Zhu, J. Zhou, D. Diao, and X. Bao, "Frequency response enhancement by periodical nonuniform sampling in distributed sensing," *IEEE Photon. Technol. Lett.*, vol. 27, no. 20, pp. 2158–2161, Oct. 2015.

[10] H. Gabai and A. Eyal, "On the sensitivity of distributed acoustic sensing," *Opt. Lett.*, vol. 41, no. 24, pp. 5648–5651, 2016.

[11] Y. Wang, Q. Liu, D. Chen, H. Li, and Z. He, "Distributed fiber-optic dynamic-strain sensor with sub-meter spatial resolution and single-shot measurement," *IEEE Photon. J.*, vol. 11, no. 6, Dec. 2019, Art. no. 6803608.

[12] Z. Ma et al., "High performance distributed acoustic sensor based on digital LFM pulse coherent-optical time domain reflectometer for intrapulse event," *Appl. Phys. Exp.*, vol. 13, no. 1, 2020, Art. no. 012016.

[13] H. Martins, K. Shi, B. Thomsen, S. Martin-Lopez, M. Gonzalez-Herraez, and S. Savory, "Real time dynamic strain monitoring of optical links using the backreflection of live PSK data," *Opt. Exp.*, vol. 24, no. 19, pp. 22303–22318, 2016.

[14] L. Shiloh, N. Levanon, and A. Eyal, "Highly-sensitive distributed dynamic strain sensing via perfect periodic coherent codes," in *Proc. 26th Int. Conf. Opt. Fiber Sensors*, 2018, Paper TuE25. [Online]. Available: https://opg.optica.org/abstract.cfm?URI=OFS-2018-TuE25

[15] C. Dorize, E. Awwad, and J. Renaudier, "High sensitivity φ-OTDR over long distance with polarization multiplexed codes," *IEEE Photon. Technol. Lett.*, vol. 31, no. 20, pp. 1654–1657, Oct. 2019.

[16] Z. Wang et al., "Distributed acoustic sensing based on pulse-coding phase-sensitive OTDR," *IEEE Internet Things J.*, vol. 6, no. 4, pp. 6117–6124, Aug. 2019.

[17] Y. Wu, Z. Wang, J. Xiong, J. Jiang, and Y. Rao, "Bipolar-coding Φ-OTDR with interference fading elimination and frequency drift compensation," *J. Lightw. Technol.*, vol. 38, no. 21, pp. 6121–6128, Nov. 2020.

[18] P. Li et al., "Random coding method for coherent detection φ-OTDR without optical amplifier," *Opt. Lasers Eng.*, vol. 161, 2023, Art. no. 107318.

[19] Y. Liang et al., "Optical-pulse-coding phase-sensitive OTDR with mismatched filtering," *Sci. China Inf. Sci.*, vol. 65, no. 9, 2022, Art. no. 192303.

[20] Y. Wu, Z. Wang, J. Xiong, J. Jiang, S. Lin, and Y. Chen, "Interference fading elimination with single rectangular pulse in Φ-OTDR," *J. Lightw. Technol.*, vol. 37, no. 13, pp. 3381–3387, Jul. 2019.

[21] D. Chen, Q. Liu, and Z. He, "High-fidelity distributed fiber-optic acoustic sensor with fading noise suppressed and sub-meter spatial resolution," *Opt. Exp.*, vol. 26, no. 13, pp. 16138–16146, 2018.

[22] D. Hilbert, *Grundzüge Einer Allgemeinen Theorie Der Linearen Integralgleichungen*, Leipzig, Germany: B.G. Teubner, 1912.

[23] H. Liang, Y. Lu, C. Li, X. Wang, and X. Zhang, "Study on decoding method of correlation coded pulses based brillouin optical time-domain reflectometric system," *Acta Optica Sinica*, vol. 31, no. 10, 2011, Art. no. 1006002.

[24] S. Lin, Z. Wang, J. Xiong, Y. Wu, and Y. Rao, "Progresses of anti-interference-fading technologies for Rayleigh-scattering-based optical fiber sensing," *Laser Optoelectron. Prog.*, vol. 58, no. 13, 2021, Art. no. 1306008.